Suppression of a pressure driven $m=1$ mode in a lower hybrid current drive plasma by electron cyclotron heating in the WT-3 tokamak

S. Yoshimura,[a] M. Watanabe,[b] K. Tanabe,[c] A. Nakayama,[d] M. Asakawa, T. Maehara,[e] M. Nakamura,[f] H. Tanaka,[g] T. Maekawa,[g] and Y. Terumichi
Department of Physics, Graduate School of Science, Kyoto University, Kyoto 606-8502, Japan

(Received 16 July 1999; accepted 6 October 1999)

A pressure driven $m=1/n=1$ mode is excited by lower hybrid current drive in the WT-3 tokamak [T. Maehara *et al.*, Nucl. Fusion **38**, 39 (1998)]. The excitation of the mode is accompanied with the decrease of the magnetic shear and with the peaking of the soft x-ray emissivity profile inside the $q=1$ surface. The crescent-shaped mode structure appeared on the contour map of the soft x-ray emissivity is consistent with that of the quasi-interchange mode. The $m=1$ mode can be suppressed by electron cyclotron heating near the $q=1$ surface. The range of the location of the electron cyclotron resonance layer effective for the complete suppression is much wider and the time scale for the suppression is much faster than those in the case of the suppression of the tearing mode in the ohmic heating plasma. © *2000 American Institute of Physics.* [S1070-664X(00)03301-2]

I. INTRODUCTION

Suppressions of low mode number magnetohydrodynamic (MHD) activities in tokamaks have long been the subject of intense study, related to the suppression of the major disruption and the improvement of the confinement. It is noticeable that electron cyclotron heating (ECH) yields a well-localized modification of the electron temperature profile near the electron cyclotron resonance (ECR) layer. Therefore, ECH is a powerful tool to suppress MHD instabilities in tokamaks.

In these ten years, ECH has been found to suppress MHD activities effectively in many tokamaks.[1–11]

The sawtooth oscillations were suppressed by applying ECH at the $q=1$ surface in DIII-D[1] and WT-3.[2,3] In WT-3, the suppression was ascribed to a modification of the current profile in such a manner as to lower the magnetic shear locally at the $q=1$ surface.[2]

On the other hand, the effectiveness of ECH for the suppression of the classical $m=2/n=1$ tearing mode, which was driven by the gradient of the plasma current at the $q=2$ surface, has been pointed out by theoretical calculations.[12–15] The $m=2$ tearing mode suppression was observed when the ECR layer was located on a narrow region near the $q=2$ surface in Tokamak-10 (T-10),[5] Jaeri Fusion Torus-2M (JFT-2M)[7] and WT-3.[10,11] A possible mechanism of the suppression was the current profile modification in the vicinity of the $q=2$ surface through the modified plasma conductivity by ECH.[9,12,13] In JFT-2M,[8] direct ECH of the O-point of the $m=2$ tearing mode was quite effective to avoid a major disruption.

Recently, neoclassical tearing modes were observed in neutral beam heated super shots on Tokamak Fusion Test Reactor (TFTR) and they caused a strong deterioration in the plasma performance.[16] Their excitation was related to the neoclassical current which was driven by a pressure gradient in the high beta plasma.[17] In a recent experiment on Axial Symmetric Divertor Experiment Upgrade (ASDEX Upgrade),[18] electron cyclotron current drive (ECCD) at the O-point was found to be effective to suppress the neoclassical tearing mode. Similarly, various pressure driven MHD instabilities were observed in tokamaks[19–21] and they have attracted attention related to the confinement. However, there was no experiment to control pressure driven MHD instabilities except for that in ASDEX Upgrade.

In WT-3, an $m=1/n=1$ mode is excited by applying lower hybrid current drive (LHCD) in an ohmic heating (OH) plasma. The excitation of the mode is accompanied with the decrease of the magnetic shear and with the peaking of the soft x-ray (SXR) intensity profile inside the $q=1$ surface, suggesting that this mode is a pressure driven mode. This mode resembles those observed in Princeton Large Torus (PLT)[22] and ASDEX[23] where the current profile was flattened in the central region and the electron temperature profile was fairly peaked by applying LHCD. In WT-3, ECH is found to be quite effective for the suppression of the pressure driven $m=1$ mode in the LHCD plasma. The range of the location of the ECR layer effective for the complete suppression is much wider compared with that in the previous suppression experiment of the $m=1$ and $m=2$ tearing modes in the OH plasma.[10,11] In addition, the time scale for the suppression of the pressure driven $m=1$ mode is much

[a]Electronic mail: yosimura@ppl.eng.osaka-u.ac.jp Permanent address: Plasma Physics Laboratory, Graduate School of Engineering, Osaka University, 2-1 Yamada-oka, Suita, Osaka 565-0871, Japan.
[b]Present address: NEC Corp., Tokyo 183-8501, Japan.
[c]Present address: Asahi Chemical Industry Corp., Shizuoka 416-8501, Japan.
[d]Present address: Toshiba Corp., Yokohama 247-8585, Japan.
[e]Permanent address: Department of Physics, Faculty of Science, Ehime University, Ehime 790-8577, Japan.
[f]Permanent address: Osaka Institute of Technology, Osaka 535-8585, Japan.
[g]Permanent address: Graduate School of Energy Science, Kyoto University, Kyoto 606-8501, Japan.

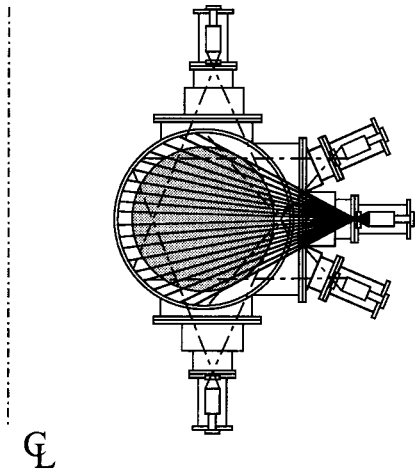

FIG. 1. The arrangement of five soft x-ray detector arrays for computerized tomography in the minor cross section. The hatched region represents the plasma.

faster than those for the suppression of the $m=1$ and $m=2$ tearing modes. These results suggest that the suppression mechanism of the pressure driven $m=1$ mode in the LHCD plasma is different from that of the previous suppression experiment on the $m=1$ and $m=2$ tearing modes in the OH plasma.

In Sec. II, we will describe the experimental apparatuses. The experimental results will be shown in Sec. III, discussed in Sec. IV, and summarized in Sec. V.

II. EXPERIMENTAL APPARATUS

The experiments are carried out in the WT-3 tokamak, with major and minor radii of $R_0=65$ cm and $a=20$ cm, respectively. The toroidal magnetic field at $R=R_0$ is $B_T \leqslant 1.75T$. The radio frequency (rf) power for LHCD is generated with a klystron amplifier ($f_{\mathrm{LHCD}}=2$ GHz, $P_{\mathrm{LHCD}} \leqslant 350$ kW) and injected into the plasma via two stacked four-waveguide launchers with a waveguide phasing of $\Delta\phi=\pi/2$. The parallel refractive index of the launched LH waves is in the range of $N_{\parallel}=1-6$ for the upper launcher and $N_{\parallel}=1-4.2$ for the lower one (Fig. 1 of Ref. 24). The power source of ECH is an 89 GHz gyrotron ($P_{\mathrm{ECH}} \leqslant 150$ kW). Microwaves from the gyrotron are transferred through a quasi-optical transmission line as a Gaussian beam and injected into the torus from the low field side using a focusing mirror in order to concentrate the ECH power around the plasma center. The launching angle is perpendicular to the toroidal magnetic field and the excited EC wave propagates in X-mode and is absorbed at the second-harmonic ECR layer, $R_{\omega=2\Omega_e}$.

The MHD activities are detected by magnetic probes and SXR detectors. Four sets of magnetic probe arrays are installed 90° apart from each other around the torus. Each array has 12 magnetic probes which surround the plasma poloidally. In order to investigate the internal MHD activities in detail, we install five SXR detector arrays which surround the plasma poloidally as shown in Fig. 1. Each array has 20 detectors sensitive to SXR in the photon energy range of $h\nu=0.2-27$ keV. The spatial structure of the SXR emissivity is reconstructed by computerized tomography (CT).[25] The other three SXR detector arrays at different toroidal locations are used for the measurement of the toroidal mode number of MHD oscillations.

III. EXPERIMENTAL RESULTS

A. Excitation of a pressure driven $m=1$ mode by LHCD

The OH plasmas with the safety factor of $q_L \simeq 3$ at the limiter and the line averaged electron density of $\overline{n_e} \simeq 0.7 \times 10^{13}\,\mathrm{cm}^{-3}$ are used for the target plasma. Figure 2 shows a typical shot for the excitation of a pressure driven $m=1$ mode by LHCD. The temporal evolution of plasma current

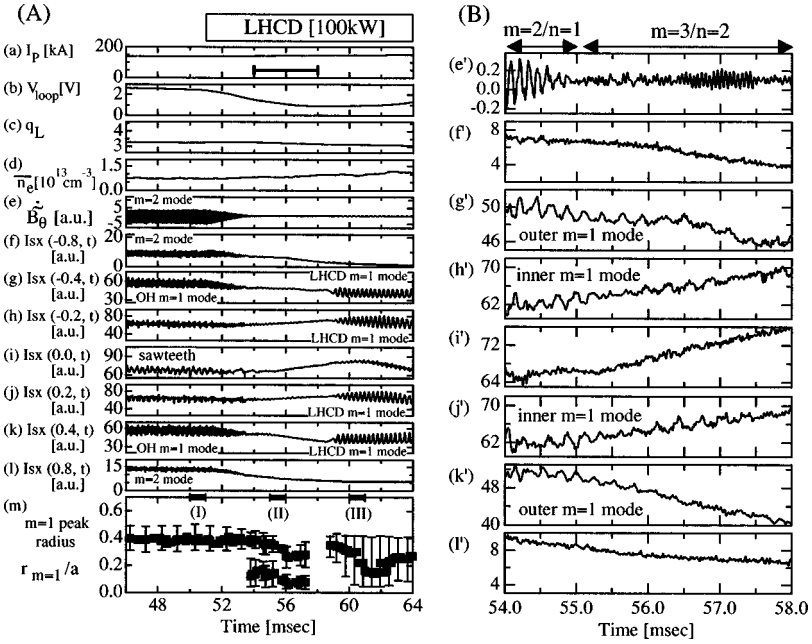

FIG. 2. (A) Waveforms of (a) plasma current I_P, (b) loop voltage V_{loop}, (c) safety factor q_L at the limiter, (d) line averaged electron density $\overline{n_e}$ along the vertical chord at $R_0=65$ cm, the center of the vacuum vessel and (e) a magnetic probe signal. LHCD ($P_{\mathrm{LHCD}}=100$ kW) is applied after 51 msec. The temporal evolution of the reconstructed soft x-ray emissivity, $I_{\mathrm{SX}}(r/a,t)$, at local locations r along the major radius across the magnetic axis is shown in (f)–(l). The temporal evolution of the radius and the width of the $m=1$ mode is shown in (m). The closed squares show the location of the peak of the $m=1$ mode. The vertical bars represent the full width at half-maximum of the $m=1$ mode structure. (B) Figures (e′)–(l′) show waveforms in (e)–(l) on an extended scale in the time window, indicated by the horizontal bar in the figure (a).

[Fig. 2(a)], loop voltage [Fig. 2(b)], safety factor q_L [Fig. 2(c)], line averaged electron density [Fig. 2(d)] and a magnetic probe signal [Fig. 2(e)] is shown. Figures 2(f)–2(l) show the time evolution of the local SXR emissivity reconstructed by the SXR CT, $I_{SX}(r/a,t)$, at several points r along the major radius across the magnetic axis. Here, $r=R-R_C$ and $R_C(=66.5\,\mathrm{cm})$ is the plasma center estimated from the magnetic measurement[26] and the SXR profile.

Before LHCD, a stationary excited $m=2/n=1$ mode is observed on the magnetic probe signal [Fig. 2(e)]. The frequency is $f\simeq 8$ kHz and the amplitude is as large as $\tilde{B}_\theta/\overline{B}_\theta \simeq 10^{-2}$. Here, $\overline{B}_\theta$ denotes the time averaged value. This mode can be also observed on $I_{SX}(\pm 0.8,t)$ [Figs. 2(f) and 2(l)]. There is also an $m=1/n=1$ mode[10,11] at $|r|/a\simeq 0.4$ [Figs. 2(g) and 2(k)]. It has the exactly same frequency as that of the $m=2$ mode. The oscillation amplitude of the $m=1$ mode is comparable with that of the $m=2$ mode [$\tilde{I}_{SX}(\pm 0.4,t)/\tilde{I}_{SX}(\pm 0.8,t)\simeq 2.5$, where $\tilde{I}_{SX}=I_{SX}-\overline{I}_{SX}$ and the over bar on I_{SX} denotes the time averaging over 1 msec]. In addition to the $m=1$ and $m=2$ modes, a sawtooth oscillation is observed on $I_{SX}(0.0,t)$, as shown in Fig. 2(i). The amplitude of the sawtooth oscillation is smaller than that of the $m=1$ mode.

By the application of LHCD, the loop voltage decreases from $V_{loop}=2.4$ to 1.0 V [Fig. 2(b)]. The plasma current and q_L are kept nearly constant [Figs. 2(a) and 2(c)]. About 60% of the total plasma current is replaced by the LH driven current. The line averaged electron density increases gradually during LHCD from $\overline{n_e}=0.7\times 10^{13}\,\mathrm{cm}^{-3}$ to $1.1\times 10^{13}\,\mathrm{cm}^{-3}$, as shown in Fig. 2(d).

In accordance with the decrease of V_{loop} by LHCD, the amplitude of $m=1$, $m=2$ and sawtooth oscillations decreases [Figs. 2(e)–2(g), 2(i), 2(k), and 2(l)]. The MHD activities look quiescent during the time $t=54-58$ msec in Figs. 2(e)–2(l). Actually, weak MHD activities are observed on I_{SX} signals as well as magnetic probe signals. Figures $(e')\sim(l')$ in Fig. 2(B) show (e)–(l) in Fig. 2(A), respectively, on an extended vertical scale as well as on an extended time scale in the time window, indicated by a horizontal bar in Fig. 2(a). It is found that there are two $m=1/n=1$ oscillations. One is observed on the inner SXR signals, $I_{SX}(\pm 0.2,t)$ [Figs. 2(h′) and 2(j′)] and the other is on the outer signals $I_{SX}(\pm 0.4,t)$ [Figs. 2(g′) and 2(k′)]. The oscillations of the inner and the outer $m=1$ modes are exactly out of phase. The amplitude of both modes is very weak ($\tilde{I}_{SX}/\overline{I}_{SX}=0.02$) compared to that of the OH $m=1$ mode ($\tilde{I}_{SX}/\overline{I}_{SX}=0.12$). No MHD oscillation is observed on the peripheral $I_{SX}(\pm 0.8,t)$ signals [Figs. 2(f′) and 2(l′)] and the central $I_{SX}(0.0,t)$ signal [Fig. 2(i′)]. On a magnetic probe signal [Fig. 2(e′)], a weak $m=3/n=2$ oscillation ($\tilde{B}_\theta/\overline{B}_\theta \simeq 10^{-4}$) appears after the complete suppression of the $m=2$ mode.

Following this, a new $m=1/n=1$ MHD oscillation with a frequency of $f\simeq 3$ kHz suddenly appears [Figs. 2(g)–2(k)]. Hereafter, we refer to this $m=1$ mode as the LHCD $m=1$ mode in distinction from the OH $m=1$ mode. The oscillation amplitude of the LHCD $m=1$ mode at $|r|/a\simeq 0.4$ [Figs. 2(g) and 2(k)] quickly grows and saturates in about one period of the oscillation and then becomes stationary. On the contrary, the oscillation amplitude on the SXR signals at $|r|/a\simeq 0.2$ gradually increases after the onset and reaches the maximum around $t=61-62$ msec as shown in Figs. 2(h) and 2(j).

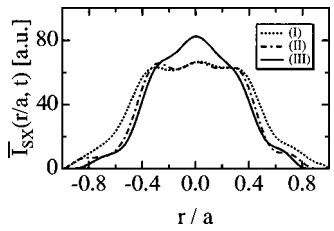

FIG. 3. Reconstructed soft x-ray profiles, $\overline{I}_{SX}(r/a,t)$, at the time marked by the characters (I), (II) and (III) in Fig. 2 (m). The typical profile in the OH plasma is shown by the curve (I). Profiles about 5 and 10 msec after LHCD on are shown by the curves (II) and (III), respectively. In order to remove fluctuation components on the soft x-ray profile, each profile is time averaged during the period which is shown by thick horizontal bars in Fig. 2(m).

We can find the radius of the peak amplitude ($r_{m=1}$) and the width of the $m=1$ mode structure from the $\tilde{I}_{SX}(r/a,t)$ radial profiles. The temporal evolution of $r_{m=1}/a$ is shown in Fig. 2(m). The vertical bars represent the full width at half-maximum of the $m=1$ mode structure. In the OH plasma, the $m=1$ mode is localized around $r_{m=1}/a\simeq 0.38$ and the width of the mode is kept constant until applying LHCD. The radius $r_{m=1}$ is considered to be near the $q=1$ surface. We cannot measure the inversion radius of the sawtooth collapse due to the large amplitude of the $m=1$ mode. Therefore, we apply the biorthogonal decomposition[27] to the SXR detector signals and separate the $m=1$ mode and the sawteeth. It is found that the inversion radius of the sawtooth collapse is equal to the radius $r_{m=1}$. Therefore, we refer to $r_{m=1}$ of the OH plasma as the original $q=1$ radius for convenience. After LHCD on, the OH $m=1$ mode is suppressed and a double $m=1$ mode structure is observed. The locations of the inner and the outer modes change temporally, as shown in Fig. 2(m). Therefore, the amplitude of the two $m=1$ oscillations on the local SXR emissivity signals [Figs. 2(g′), 2(h′), 2(j′), and 2(k′)] does not have a steady value during this time. Then, the double $m=1$ mode disappears and after short time interval the LHCD $m=1$ mode appears. After the appearance, the width of the mode expands gradually and it saturates around $t=60$ msec. The width of the LHCD $m=1$ mode extends from the plasma axis to the radial position of $|r|/a\simeq 0.4$. The LHCD $m=1$ mode is found to share the entire interior domain of the original $q=1$ surface. On the contrary, the OH $m=1$ mode is localized at the original $q=1$ surface. The internal structure of the LHCD $m=1$ mode is quite different from that of the OH $m=1$ mode.

The SXR profile changes in accordance with the change of the MHD activities. In Fig. 3, the $\overline{I}_{SX}(r/a,t)$ profiles at the time marked by characters (I), (II) and (III) in Fig. 2(m) are shown by three curves. The typical SXR profile in the OH plasma is shown by the curve (I) in Fig. 3. The curve (II) in Fig. 3 shows the profile at about 5 msec after applying LHCD when the double $m=1$ mode structure is observed.

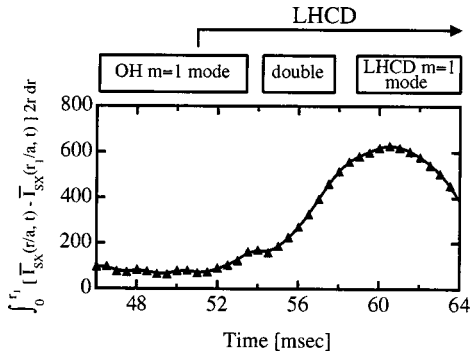

FIG. 4. The temporal evolution of the integral of $\overline{I}_{SX}(r/a,t)-\overline{I}_{SX}(r_1/a,t)$ inside the $q=1$ surface. Here, r_1 is the radius of the original $q=1$ surface.

The curve (III) in Fig. 3 shows the profile when the width of the LHCD $m=1$ mode expands most. It is found that the target OH plasma has a flat profile near the center. After applying LHCD, the SXR intensity outside the original $q=1$ surface begins to decrease, while the central profile is not so changed and keeps a flat profile for a while, as shown by the curve (II) in Fig. 3. After the time (II), the central SXR intensity begins to increase [Fig. 2(i)] and finally a peaked profile is produced [the curve (III) in Fig. 3] inside the original $q=1$ surface and the LHCD $m=1$ mode appears.

It is found that the excitation of the LHCD $m=1$ mode is closely related to the peaking of the $\overline{I}_{SX}$ profile inside the original $q=1$ surface. Therefore, it may be the case that the LHCD $m=1$ mode is excited by the increase of β_{p1}. Here, β_{p1} is the poloidal beta inside the $q=1$ surface and is defined as follows.[28]

$$\beta_{p1}=\frac{\int_0^{r_1}[p(r)-p(r_1)]2r\,dr}{[B_\theta(r_1)^2/2\mu_0]r_1^2}. \tag{1}$$

Here, $p(r)$ is the pressure profile, r_1 is the radius of the $q=1$ surface and B_θ is the poloidal magnetic field. As a measure of β_{p1}, we calculate the numerator of the equation (1) with replacing the pressure profile $p(r)$ by the $\overline{I}_{SX}(r/a,t)$ profile, on the assumption that the pressure profile $p(r)$ is proportional to the $\overline{I}_{SX}(r/a,t)$ profile. The calculation is the integral of $\overline{I}_{SX}(r/a,t)-\overline{I}_{SX}(r_1/a,t)$ inside the $q=1$ surface and it is defined as follows:

$$\int_0^{r_1}[\overline{I}_{SX}(r/a,t)-\overline{I}_{SX}(r_1/a,t)]2r\,dr. \tag{2}$$

Here, we use the radius of the original $q=1$ surface for r_1. The time evolution of the integral of the equation (2) is shown in Fig. 4. After applying LHCD, the central $\overline{I}_{SX}(r/a,t)$ profile keeps nearly flat for a while, so the integral of the equation (2) increases only slightly. After 55 msec, it begins to increase clearly. Then, the LHCD $m=1$ mode appears.

The radial profile of the electron density in the range $|r|/a=0-0.7$ is measured by a HCN laser interferometer. The electron density increases over the whole area during LHCD, maintaining the same profile. It was found empirically that in these experimental conditions on WT-3 there was almost linear relation between the electron temperature and the SXR intensity[29] if the density was kept constant. In addition, we have measured the electron temperature of a similar LHCD plasma accompanied with the LHCD $m=1$ mode by a Thomson scattering apparatus. The electron temperature at the plasma center increased slightly ($T_e=600\rightarrow700$ eV just after the excitation of the LHCD $m=1$ mode), while that at $r/a=0.5$ decreased ($T_e=400\rightarrow150$ eV).[30] These results indicate that the peaking of the $\overline{I}_{SX}$ profile during LHCD represents the peaking of the electron temperature profile rather than the impurity accumulation. Therefore, it may be reasonable to use the value evaluated from the equation (2) for the study of the time evolution of β_{p1} as shown in Fig. 4.

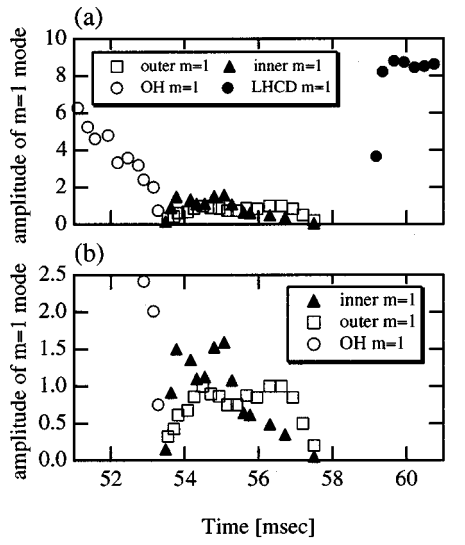

FIG. 5. (a) The change of the amplitude of the $m=1$ mode after applying LHCD. (b) The change of the amplitude of the $m=1$ mode is shown with the enlarged vertical scale.

Although we do not measure the current profile directly, the change of the q profile can be suggested from the behavior of the $m=1$ mode. The time evolution of the amplitude of the $m=1$ mode after applying LHCD is shown in Fig. 5(a). In Fig. 5(b), it is shown with the enlarged vertical scale to enhance the visibility of the temporal evolution of the double $m=1$ mode. After applying LHCD, the amplitude of the OH $m=1$ mode is reduced, as shown in Fig. 5(a). After 53.5 msec, the inner $m=1$ mode appears in addition to the outer $m=1$ mode. The amplitudes of both $m=1$ modes begin to increase and saturate with small amplitude [Fig. 5(b)]. The appearance of the double $m=1$ mode indicates that the safety factor at the magnetic axis, q_0, increases to be $q_0>1$ and there are two $q=1$ surfaces after 53.5 msec. Therefore, the magnetic shear seems to be reversed in the central region. After 56 msec, the amplitude of the inner $m=1$ mode and then that of the outer $m=1$ mode start to decrease. On the other hand, only small change of the $r_{m=1}$ of both modes is observed during 56–58 msec, as shown in Fig. 2(m). Finally, both modes disappear completely at about 58 msec. During 58–59 msec, no $m=1$ mode is observed on the SXR

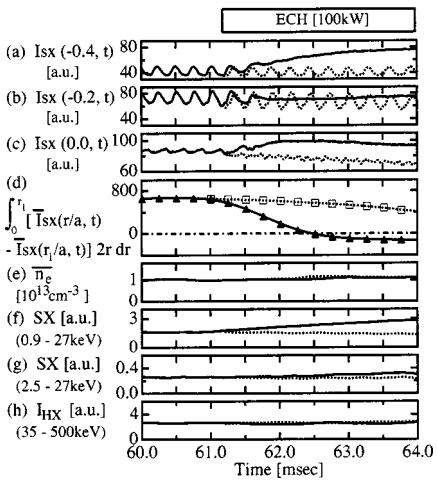

FIG. 6. Waveforms of plasma parameters of a typical shot with (solid line) and without (dashed line) ECH. (a)–(c) The temporal evolution of reconstructed soft x-ray signals I_{SX} at $r/a=-0.4,-0.2$ and 0.0. ECH ($P_{ECH}=100$ KW) is applied after 61.2 msec to the LHCD plasma. (d) The time evolution of the integral of $\overline{I}_{SX}(r/a,t)-\overline{I}_{SX}(r_1/a,t)$ inside the original $q=1$ surface is shown by closed triangles (with ECH) and open squares (without ECH). The others are waveforms of (e) line averaged electron density $\overline{n_e}$, (f) soft x-ray detector signals which are viewing the whole plasma column and are sensitive to 0.9–27 keV (g) 2.5–27 keV, and (h) a hard x-ray signal I_{HX} which has a viewing chord through the plasma center.

signals. These results suggest that after 56 msec the magnetic shear at the two $q=1$ surfaces begins to decrease without changing the location of the $q=1$ surfaces and the q_0 begins to decrease to be $q_0\simeq 1$. The q profile in the central region seems to become flat with $q\simeq 1$ before the appearance of the LHCD $m=1$ mode. On the other hand, the $m=2$ mode is completely suppressed by LHCD, suggesting that the current gradient at the $q=2$ surface may be reduced. These change of the current profile in both the central region and the peripheral region will result in the steepening of the current profile near the $q=1.5$ surface. This is one of the plausible accounts for the appearance of the $m=3/n=2$ oscillation.

The flattening of the current profile and the peaking of the $\overline{I}_{SX}$ profile inside the original $q=1$ surface just before the onset of the LHCD $m=1$ mode suggest that this mode is driven by the pressure rather than the current gradient. In addition, the time interval between the disappearance of the double $m=1$ mode and the excitation of the LHCD $m=1$ mode is much shorter (~ 1 msec) than the time scale of the global change of the current profile (~ 10 msec). Therefore, it seems to be reasonable that the current profile in the central region keeps flat even after the excitation of the LHCD $m=1$ mode and the excitation cannot be ascribed to the steepening of the current gradient.

B. Suppression of the pressure driven $m=1$ mode by ECH

Figure 6 shows a typical shot for the suppression of the LHCD $m=1$ mode by ECH. Here, the ECR layer is located at $|r|/a=0.34$ in the high field side and ECH is turned on at the time when the LHCD $m=1$ mode expands most. After ECH on, the mode is suppressed quickly in about two periods of the oscillation (~ 0.5 msec) [Figs. 6(a) and 6(b)] as

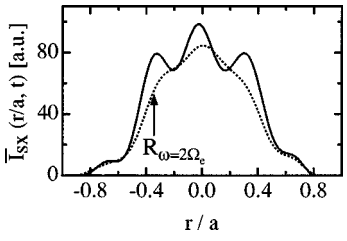

FIG. 7. Reconstructed soft x-ray profiles, $\overline{I}_{SX}(r/a,t)$, with (solid line) and without (dashed line) ECH. The location of the ECR layer is indicated by an arrow.

the integral of the equation (2) is decreasing [Fig. 6(d)]. When the LHCD $m=1$ mode is completely suppressed, the $\overline{I}_{SX}$ increases at the plasma center as well as at the ECR layer as shown in Fig. 7. The gradient on the $\overline{I}_{SX}$ profile, $d\overline{I}_{SX}(r/a,t)/d|r|$, become positive around $|r|/a\simeq 0.25$.

The hard x-ray intensity I_{HX}, in the range of $h\nu=35-500$ keV, does not change by ECH as shown in Fig. 6(h). Four SXR detectors viewing the whole plasma column are installed. They have Be foils of different thicknesses by which the manifestation of the microwave absorption by tail or bulk electrons can be checked. They are sensitive to SXR in the range of 0.2–27, 0.9–27, 1.7–27 and 2.5–27 keV with more than 10% detection efficiency. Although the SXR signals of 0.2–27 and 0.9–27 keV clearly increase [Fig. 6(f)], those of 1.7–27 and 2.5–27 keV increase only slightly [Fig. 6(g)]. The line averaged density does not change as shown in Fig. 6(e). These results indicate the bulk electron heating by ECH.

The ray tracing calculation shows that the single pass absorption of the EC wave is about 60% under the experimental condition. The profiles of the electron density and temperature of the target plasma are assumed to be $n_e(r)=n_{e0}(1-r^2/a^2)$ and $T_e(r)=T_{e0}(1-r^2/a^2)$ in the calculation, where $T_{e0}=400$ eV, $n_{e0}=1.0\times 10^{13}\,\mathrm{cm}^{-3}$ and $B_T=1.47$ T.

Responses of the LHCD $m=1$ mode for the various locations of the ECR layer are investigated systematically. The location of the ECR layer is scanned by changing both B_T and I_P with q_L to be kept constant. The complete suppression is obtained when the ECR layer is located in the range of $|r|/a\simeq 0.27-0.40$ as shown in Fig. 8(a). It is noted that the time needed for the complete suppression after ECH on is in the range of $t\simeq 0.4-0.75$ msec and depends only weakly on the location of the ECR layer as shown in Fig. 8(b). When the ECR layer is located in this region, the positive gradient on the $\overline{I}_{SX}$ profile is always observed and the integral of the equation (2) is decreased. When the ECR layer is positioned near the center of the plasma or in the $|r|/a\geqslant 0.5$ region, there is no suppression of the LHCD $m=1$ mode. In this case, the decrease of the integral of the equation (2) is not observed.

IV. DISCUSSIONS

The excitation of the LHCD $m=1/n=1$ mode is accompanied with the decrease of the magnetic shear and with the

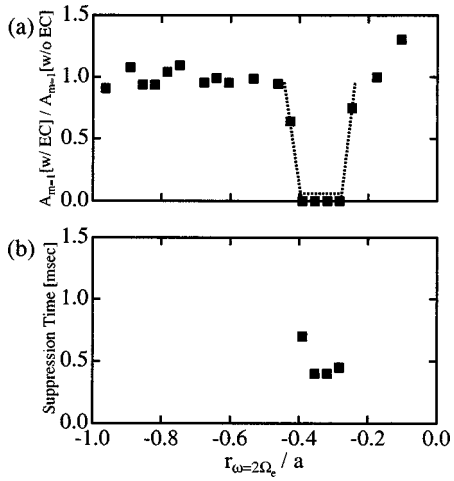

FIG. 8. (a) The oscillation amplitude ratio of the case with ECH (1 msec after ECH on) and that without ECH for the LHCD $m=1$ mode is plotted as the function of the location of the ECR layer $r_{\omega=2\Omega_e}$. The oscillation amplitude is measured by the soft x-ray detector which has the viewing chord tangential to the peak location of the LHCD $m=1$ mode. The scan of the ECR layer is carried out in the range $|r_{\omega=2\Omega_e}| / a=0.10-0.96$ in the high field side. The LHCD power (100 kW) and the ECH power (100 kW) is held constant during the scan. (b) The required time for the complete suppression of the LHCD $m=1$ mode is shown.

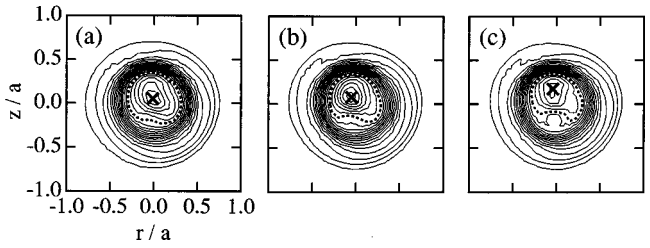

FIG. 9. The contour maps of the soft x-ray emissivity of the LHCD plasma in the minor cross-section at (a) 60.1 msec, (b) 61.7 msec and (c) 63.4 msec. The mark ''×'' in each figure shows the position of the peak of the soft x-ray emissivity.

peaking of the $\overline{I}_{SX}$ profile inside the original $q=1$ surface, which suggests that this mode is a pressure driven mode. One of possible candidates for the identity of the pressure driven $m=1/n=1$ mode is the internal kink mode. The internal kink mode is excited by the pressure inside the $q=1$ surface and for the excitation it requires $\beta_{p1}\geqslant 0.3$ for the usual current profile.[28] However, in the present experimental condition β_{p1} is estimated to be as low as ≈ 0.02, which is much less than the threshold for the excitation of the internal kink mode. Therefore, at first glance the internal kink mode may be excluded from candidates for the identity of the LHCD $m=1$ mode. On the other hand, it was theoretically shown that when the q profile became flat inside the $q=1$ surface with $q_0\simeq 1$ at the magnetic axis, the critical β_{p1} required for the instability was reduced.[31] In this case, the plasma displacement accompanied with the instability takes the form of a convection of the quasi-interchange type rather than a rigid shift.

Since the magnetic shear is found to be reduced before the excitation of the LHCD $m=1$ mode, this ''quasi-interchange'' mode may be the case. We investigate the time evolution of the internal mode structure of the LHCD $m=1$ mode on the contour map of the SXR emissivity, as shown in Figs. 9(a)–9(c). The point ''×'' in each figure shows the location of the peak of the SXR emissivity. One of the contours is shown by the dashed line in each figure. Although just after the mode onset the shift of the ''×'' point is small, as shown in Fig. 9(a), the dashed contour is somewhat distorted. The shift of the ''×'' point gradually increases, as shown in Figs. 9(b) and 9(c), and the shape of the dashed contour becomes crescent. Such a crescent shape is a distinctive characteristic of the quasi-interchange mode.[31]

The fact that the LHCD $m=1$ mode is not a resistive instability seems appear in the experimental results on the suppression by ECH. Namely, the range of the location of the ECR layer where the complete suppression is obtained is much wider ($\Delta r/a\simeq 0.13$) compared with the previous cases of the suppression experiments of the tearing modes ($\Delta r/a\simeq 0.05$)[10,11] and sawtooth oscillations ($\Delta r/a\simeq 0.03$)[2,3] in OH plasmas by ECH. It is also wider than the width of the deposition profile of the ECH power ($\delta r/a\simeq 0.04$). In addition, the time scale for the suppression of the LHCD $m=1$ mode is much faster (~ 0.5 msec) than that for the tearing modes in the OH plasma (~ 2 msec). If the suppression by ECH is due to the current profile modification, for the complete suppression it may take a time corresponding to the current diffusion time defined by a formula, $\tau=\mu_0(dr)^2/\eta$, where η is the parallel resistivity near the $q=1$ surface and dr is the length from the heating layer to the $q=1$ surface. Here τ is estimated to be ≈ 1.3 msec with $dr=\Delta r/2$ using the present experimental condition of $T_e=400$ eV and $Z_{\text{eff}}=2$. The estimated time scale is on the same order as the experimental results of the suppression time of the LHCD $m=1$ mode. However, if the suppression is due to the current profile modification, the suppression time will depend on $(dr)^2$. However, there is no such strong dependence of the suppression time on the location of the ECR layer in Fig. 8(b). These results suggest that the suppression cannot be ascribed to the current profile modification. On the contrary, the integral of the equation (2) [Fig. 6(d)] begins to decrease immediately after ECH on, indicating that the suppression is ascribed to the modification of the pressure profile inside the $q=1$ surface.

Another distinctive feature of the present experiment of the mode suppression is the shape of the dip denoted by a dotted line in Fig. 8(a), which takes a form of the figure ''U.'' In the suppression experiment of the OH tearing mode by ECH, on the contrary, the suppression dip takes a form of the figure ''V,'' that is, the complete suppression is obtained only at the ECR location corresponding to the bottom of the figure ''V.''[5,7,10,11] When the location of the ECR layer is outside of this very point, only incomplete suppression is obtained. A computer simulation[15] suggested that this character was ascribed to the location of EC heating zone on the magnetic island of the tearing mode. Namely, if the EC heating layer is just on the O-point, a complete suppression may be obtained. On the other hand, when the heating layer is

located outside the O-point, the width of the magnetic island will shrink. However, the shrinking will be stopped when the heating layer becomes outside of the island. Thus, the suppression dip of the figure ''U'' seems to be inconsistent with the tearing type instability.

Similar stationary excited $m=1$ modes were observed in LHCD plasmas on PLT[22] and ASDEX.[23] In these tokamaks, the sawtooth oscillations could be suppressed by a modest power of LHCD; however, a stationary $m=1/n=1$ oscillation was excited in accordance with the increase of the central electron temperature and the flattening of the central current profile. The $m=1$ mode persisted even after the complete suppression of sawteeth. These results suggest that the LHCD induced $m=1$ modes in PLT and ASDEX are the same instability as that observed in WT-3 and these $m=1$ modes are the pressure driven modes. In the present paper, we show further that the internal mode structure of the LHCD $m=1$ mode is of quasi-interchange type by the SXR CT and that the mode can be stabilized by the pressure profile modification using ECH.

In a high toroidal field operation on ASDEX,[23] the LHCD induced $m=1$ mode was absent. In this case, a very high central electron temperature was observed, suggesting that the LHCD induced $m=1$ mode had a very bad effect on the plasma confinement. In the present experiment on WT-3, it is noted that the central $\overline{I_{SX}}$ increases when the LHCD $m=1$ mode is suppressed by ECH, as shown in Fig. 7. This may suggest the improvement of the confinement accompanied with the disappearance of the LHCD $m=1$ mode.

V. SUMMARY

The excitation of the LHCD $m=1$ mode is accompanied with the decrease of the magnetic shear and with the peaking of the I_{SX} profile inside the original $q=1$ surface, which suggests that this mode is driven by the pressure rather than the current gradient. The crescent-shaped mode structure appeared on the contour map of SXR emissivity is consistent with the quasi-interchange mode which can be excited when the central q profile is flat with $q_0 \simeq 1$.

The LHCD $m=1$ mode can be suppressed completely by ECH. The range of the location of the ECR layer effective for the complete suppression is much wider than that in the case of the suppression of the tearing modes in the OH plasma by ECH. The suppression dip versus the location of the ECR layer takes the form of the figure ''U'' which suggests that the suppressed mode is not a tearing mode. On the other hand, the time scale for the suppression is much faster than that in the case of the suppression of the tearing modes by ECH.

In conclusion, the quasi-interchange mode can be stabilized by the modification of the pressure profile inside the $q=1$ surface using ECH.

ACKNOWLEDGMENTS

One of the authors (S. Yoshimura) would like to thank Professor S. Goto and Professor S. Okada (Osaka University) for their encouragement. This work was partially supported by a Grant-in-Aid for Scientific Research of the Ministry of Education of Japan.

[1] R. T. Snider, D. Content, R. James, J. Lohr, M. A. Mahdavi, R. Prater, and B. Stallard, Phys. Fluids B **1**, 404 (1989).
[2] K. Hanada, H. Tanaka, M. Iida *et al.*, Phys. Rev. Lett. **66**, 1974 (1991).
[3] K. Hanada, T. Maehara, K. Makino *et al.*, Phys. Fluids B **4**, 3675 (1992).
[4] V. V. Alikaev, Yu. I. Arsentiev, A. A. Bagdasarov *et al.*, in *Plasma Physics and Controlled Nuclear Fusion Research, 1984*, London (International Atomic Energy Agency, Vienna, 1985), Vol. 1, p. 419.
[5] D. A. Kislov, V. V. Alikaev, Yu. V. Esipchuk *et al.*, Nucl. Fusion **37**, 339 (1997).
[6] TFR Group, FOM ECRH Team, Nucl. Fusion **28**, 1995 (1988).
[7] K. Hoshino, M. Mori, T. Yamamoto *et al.*, Phys. Rev. Lett. **69**, 2208 (1992).
[8] K. Hoshino, H. Aikawa, Y. Asahi *et al.*, in *Plasma Physics and Controlled Nuclear Fusion Research, 1994*, Seville (International Atomic Energy Agency, Vienna, 1995), Vol. 1, p. 697.
[9] D. C. Sing, M. E. Austin, D. L. Brower *et al.*, Phys. Fluids B **5**, 3239 (1993).
[10] S. Yoshimura, K. Hanada, Y. Kishigami *et al.*, Fusion Eng. Des. **26**, 77 (1995).
[11] Y. Terumichi, T. Maekawa, K. Hanada *et al.*, in *Plasma Physics and Controlled Nuclear Fusion Research, 1994*, Seville (International Atomic Energy Agency, Vienna, 1995), Vol. 2, p. 189.
[12] V. Chan and G. Guest, Nucl. Fusion **22**, 272 (1982).
[13] E. Westerhof and W. J. Goedheer, Plasma Phys. Controlled Fusion **30**, 1691 (1988).
[14] Y. Yoshioka, S. Kinoshita, and T. Kobayashi, Nucl. Fusion **24**, 565 (1984).
[15] G. Kurita, T. Tuda, M. Azumi, T. Takizuka, and T. Takeda, Nucl. Fusion **34**, 1497 (1994).
[16] Z. Chang, J. D. Callen, E. D. Fredrickson, R. V. Budny, C. C. Hegna, K. M. McGuire, M. C. Zarnstorff, and the TFTR group, Phys. Rev. Lett. **74**, 4663 (1995).
[17] Z. Chang, E. D. Fredrickson, S. H. Batha *et al.*, Phys. Plasmas **5**, 1076 (1998).
[18] H. Zohm, G. Gantenbein, G. Giruzzi *et al.*, Nucl. Fusion **39**, 577 (1999).
[19] R. J. La Haye, J. D. Callen, M. S. Chu *et al.*, in *Fusion Energy, 1996*, Montreal (International Atomic Energy Agency, Vienna, 1997), Vol. 1, p. 747.
[20] D. A. Gates, B. Lloyd, A. W. Morris *et al.*, in *Fusion Energy, 1996*, Montreal (International Atomic Energy Agency, Vienna, 1997), Vol. 1, p. 715.
[21] S. Günter, S. D. Pinches, A. Gude, K. Hallatschek, K. Lackner, and the ASDEX Upgrade Team, Nucl. Fusion **38**, 325 (1998).
[22] T. K. Chu, R. Bell, S. Bernabei *et al.*, Nucl. Fusion **26**, 666 (1986); S. Bernabei, R. Bell, A. Cavallo *et al.*, in *Plasma Physics and Controlled Nuclear Fusion Research, 1986*, Kyoto (International Atomic Energy Agency, Vienna, 1987), Vol. 1, p. 503.
[23] F. X. Söldner, F. Leuterer, R. Bartiromo *et al.*, Nucl. Fusion **34**, 985 (1994).
[24] T. Maekawa, M. Iida, H. Tanaka *et al.*, Nucl. Fusion **31**, 1394 (1991).
[25] Y. Nagayama, J. Appl. Phys. **62**, 2702 (1987).
[26] D. W. Swain and G. H. Neilson, Nucl. Fusion **22**, 1015 (1982).
[27] T. Dudok de Wit, A.-L. Pecquet, J.-C. Vallet, and R. Lima, Phys. Plasmas **1**, 3288 (1994).
[28] J. Wesson, *Tokamaks* (Clarendon, Oxford, 1997).
[29] K. Hanada, J. Phys. Soc. Jpn. **63**, 967 (1994).
[30] M. Nakamura, T. Minami, K. Hanada *et al.*, Nucl. Fusion **31**, 1485 (1991).
[31] J. A. Wesson, P. Kirby, and M. F. Nave, in *Plasma Physics and Controlled Nuclear Fusion Research, 1986*, Kyoto (International Atomic Energy Agency, Vienna, 1987), Vol. 2, p. 3.